LETTER

Stable and mobile two-dimensional dipolar ring-dark-in-bright Bose–Einstein condensate soliton

IOP Publishing | Astro Ltd Laser Physics Letters
Laser Phys. Lett. 13 (2016) 035502 (7pp) doi:10.1088/1612-2011/13/3/035502

Stable and mobile two-dimensional dipolar ring-dark-in-bright Bose–Einstein condensate soliton

S K Adhikari[1]

Instituto de Física Teórica, UNESP—Universidade Estadual Paulista, 01.140-070 São Paulo, São Paulo, Brazil

E-mail: Adhikari@ift.unesp.br

Received 22 December 2015
Accepted for publication 7 January 2016
Published 8 February 2016

Abstract

We demonstrate robust, stable, mobile two-dimensional (2D) dipolar ring-dark-in-bright (RDB) Bose–Einstein condensate (BEC) solitons for repulsive contact interaction, subject to a harmonic trap along the y direction perpendicular to the polarisation direction z. Such a RDB soliton has a ring-shaped notch (zero in density) imprinted on a 2D bright soliton free to move in the $x - z$ plane. At medium velocity the head-on collision of two such solitons is found to be quasi-elastic with practically no deformation. The possibility of creating the RDB soliton by phase imprinting is demonstrated. The findings are illustrated using numerical simulation employing realistic interaction parameters in a dipolar ^{164}Dy BEC.

Keywords: Bose–Einstein condensation, dipolar atoms, soliton

(Some figures may appear in colour only in the online journal)

1. Introduction

A bright soliton is a localised peak in density that can travel at a constant velocity in one dimension (1D) with its shape unchanged, due to a cancellation of nonlinear attraction and dispersive effects [1]. Similarly, a dark soliton represents a dip or notch (zero) in density in a uniform medium that can travel in 1D maintaining its shape. Bright solitons have been observed in water waves, nonlinear optics and Bose–Einstein condensate (BEC) etc, among others [1]. In the physical three-dimensional (3D) world, 1D bright solitons were observed in the BEC of ^{7}Li [2] and ^{85}Rb atoms [3].

In the absence of a uniform BEC in a laboratory to create a mobile 1D dark soliton, a notchin density in a finite trapped quasi-one-dimensional (quasi-1D) repulsive BEC along its width, dividing the BEC into two equal pieces, has been observed in a quasi-1D BEC of ^{87}Rb atoms [4–6] and termed a dark soliton. However, these dark solitons exhibit thermal and dynamical instabilities [7, 8] except for very strong transverse traps corresponding to a quasi-1D geometry. For a moderate to weak transverse confinement, the dark solitons areunstable, show snake instability [7] and decay to form a vortex ring [6]. Although the pioneering experiments on quasi-1D dark solitons [4] faced technical difficulties in their stabilisation due to thermal and dynamical effects, these problems are somewhat under control in recent investigations and the different aspects and properties of dark solitons have been studied lately [9]. The dynamical instability of dark solitons becomes explicit when the quasi-1D condition is relaxed, and the bending and snaking (dynamical) instability of dark solitons seriously hampers both theoretical and experimental studies [5, 6, 10].

A more stable variant of the dark soliton, called the ring-dark soliton, has also been suggested in a trapped repulsive BEC [11] and in a uniform self-defocusing medium in nonlinear optics [12], and later observedin optics [13]. A ring-dark soliton possesses a notch in density in the form of a ring in a quasi-two-dimensional (quasi-2D) trapped BEC, thus creating a ring-shaped concentric notch in a disk-shaped BEC. However, the ring-dark soliton created on a quasi-2D BEC is dynamically unstable in general [11], and this creates difficulty in their theoretical and experimental studies [14]. The generation of ring-dark solitons by phase engineering and their oscillations in spin-1 Bose–Einstein condensates have

[1] www.ift.unesp.br/users/Adhikari

also been studied theoretically [15]. This instability can be reduced by reducing the strength of the axial trap in a quasi-1D BEC and the in-plane trap in a quasi-2D BEC hosting the dark and ring-dark solitons, respectively. Nevertheless, the ring-dark solitons are to be created in a repulsive quasi-2D BEC and the in-plane trap can not be arbitrarily reduced as this will lead to arbitrarily large BECs hosting these solitons, thus making it impossible to observe them experimentally.

Recent observation of dipolar BECs of ^{164}Dy [16, 17], ^{168}Er [18] and ^{52}Cr [19] atoms has opened up new studies in BEC solitons. In a dipolar BEC, apart from the 1D solitons [20] free to move in a straight line, a two-dimensional (2D) soliton [21] free to move on a plane is possible. Dipolar 1D and 2D BEC solitons can be realised either by a harmonic or an optical-lattice trap in quasi-1D [22] and quasi-2D [23] settings, respectively. Robust 1D and 2D dipolar BEC solitons accommodating a large number of atoms are possible for a fully repulsive contact interaction [20]. The long-range dipolar attraction prevents the escape of the atoms from the soliton and the contact repulsion gives stability against collapse.

We demonstrated that the dynamical instability of a dark soliton can be eliminated if the dark soliton is imprinted on a 1D dipolar BEC soliton instead of on a trapped BEC [24]. Even a dynamically stable dark soliton can be realised on a 2D dipolar BEC soliton [25]. These 1D and 2D dipolar dark-in-bright solitons without any axial trap or an in-plane trap, respectively, do not exhibit bending or snaking instability of nondipolar dark solitons in a repulsive trapped BEC.

In this letter we demonstrate that a dynamically stable ring-dark soliton can be realised on a 2D bright dipolar soliton. Such a 2D dipolar ring-dark-in-bright (RDB) soliton, harmonically trapped in the y direction, is mobile on the $x-z$ plane with a constant velocity, where z is the polarisation direction. These RDB solitons are stationary excitations of the 2D dipolar bright solitons.

The statics and dynamics of the 2D dipolar RDB solitons are studied by a real-time propagation of the 2D and 3D mean-field Gross–Pitaevskii (GP) equation. The stability of these solitons is established by studying their breathing oscillation over a long time subject to a reasonable perturbation. At medium velocities, the head-on collision between two RDB solitons in real-time simulation is found to be quasi-elastic for velocities along both the x and z directions. We also study the creation of the RDB solitons by phase imprinting [4, 26] a 2D Gaussian profile by introducing a phase difference of π between parts of the BEC wave function on both sides of the dark ring.

2. Mean-field Gross–Pitaevskii equations

We consider a dipolar BEC soliton, with the mass, number of atoms, magnetic dipole moment and scattering length given by m, N, μ and a, respectively. The interaction between two atoms at $\mathbf{r}$ and $\mathbf{r}'$ is [27]

$$V(\mathbf{R}) = 3a_{\rm dd}V_{\rm dd}(\mathbf{R}) + 4\pi a\delta(\mathbf{R}), \quad \mathbf{R} = (\mathbf{r}-\mathbf{r}'), \qquad (1)$$

with

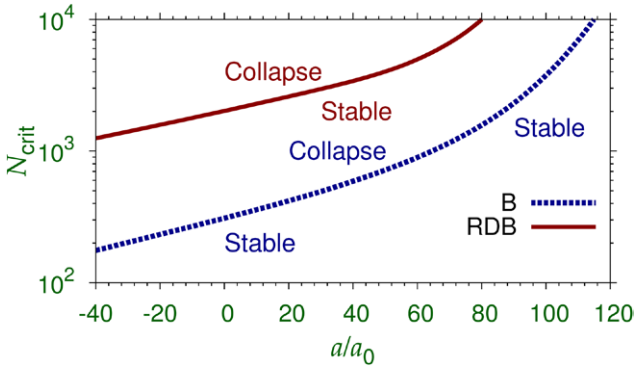

Figure 1. Critical number of ^{164}Dy atoms $N_{\rm crit}$ for the formation of a stable 2D bright (B) and RDB soliton as obtained from a solution of (4). The oscillator length $l \equiv \sqrt{\hbar/mw} = 1\,\mu$m and the dipolar length $a_{\rm dd} = 132.7a_0$. The soliton collapses for for a number of atoms $N > N_{\rm crit}$.

$$a_{\rm dd} = \frac{\mu_0\mu^2 m}{12\pi\hbar^2}, \quad V_{\rm dd}(\mathbf{R}) = \frac{1-3\cos^2\theta}{\mathbf{R}^3}, \qquad (2)$$

where μ_0 is the permeability of free space, θ is the angle made by the vector $\mathbf{R}$ with the polarisation z direction. This interaction leads to *a fully asymmetric* stable, 2D RDB soliton mobile on the $x-z$ plane in the presence of a harmonic trap along y axis. The dimensionless GP equation in this case can be written as [27, 28]

$$\mathrm{i}\frac{\partial\phi(\mathbf{r},t)}{\partial t} = \left[-\frac{\nabla^2}{2} + \frac{1}{2}y^2 + g|\phi|^2 + g_{\rm dd}\int V_{\rm dd}(\mathbf{R})|\phi(\mathbf{r}',t)|^2\,\mathrm{d}\mathbf{r}'\right]\phi(\mathbf{r},t), \qquad (3)$$

where $g = 4\pi aN$, $g_{\rm dd} = 3Na_{\rm dd}$ and $\int|\phi(\mathbf{r},t)|^2 d\mathbf{r} = 1$. In (3), the length is expressed in units of oscillator length $l = \sqrt{\hbar/(m\omega)}$, where ω is the circular frequency of the harmonic trap along the y axis. The energy is in units of oscillator energy $\hbar\omega$, the probability density $|\phi|^2$ in units of l^{-3} and time in units of $t_0 = 1/\omega$. In (3) the dipolar interaction is anisotropic on the $x-z$ plane, thus making the 2D bright and RDB solitons anisotropic on this plane.

In place of the 3D equation (3), a quasi-2D model appropriate for the quasi-2D RDB solitons of large spatial extension is very economic and convenient from a computational point of view, especially for real-time dynamics. The system is assumed to be in the ground state $\phi(y) = \exp(-y^2/2)/(\pi)^{1/4}$ of the axial trap and the wave function can be written as $\phi(\mathbf{r},t) = \phi(y)\phi_{\rm 2D}(\vec{\rho},t)$, where $\vec{\rho} \equiv \{x,z\}$ and $\phi_{\rm 2D}(\vec{\rho},t)$ is an effective wave function on the $x-z$ plane. Using this ansatz in (3), the y dependence can be integrated out to obtain the following effective 2D equation [28, 29]

$$\mathrm{i}\frac{\partial\phi_{\rm 2D}(\vec{\rho},t)}{\partial t} = \left[-\frac{\nabla_\rho^2}{2} + \frac{g}{\sqrt{2\pi}}|\phi_{\rm 2D}(\vec{\rho},t)|^2 + \frac{4\pi g_{\rm dd}}{3\sqrt{2\pi}} \times \int\frac{\mathrm{d}\mathbf{k}_\rho}{(2\pi)^2}\mathrm{e}^{-\mathrm{i}\mathbf{k}_\rho\cdot\vec{\rho}}n(\mathbf{k}_\rho,t)j_{\rm 2D}(\xi)\right]\phi_{\rm 2D}(\vec{\rho},t), \qquad (4)$$

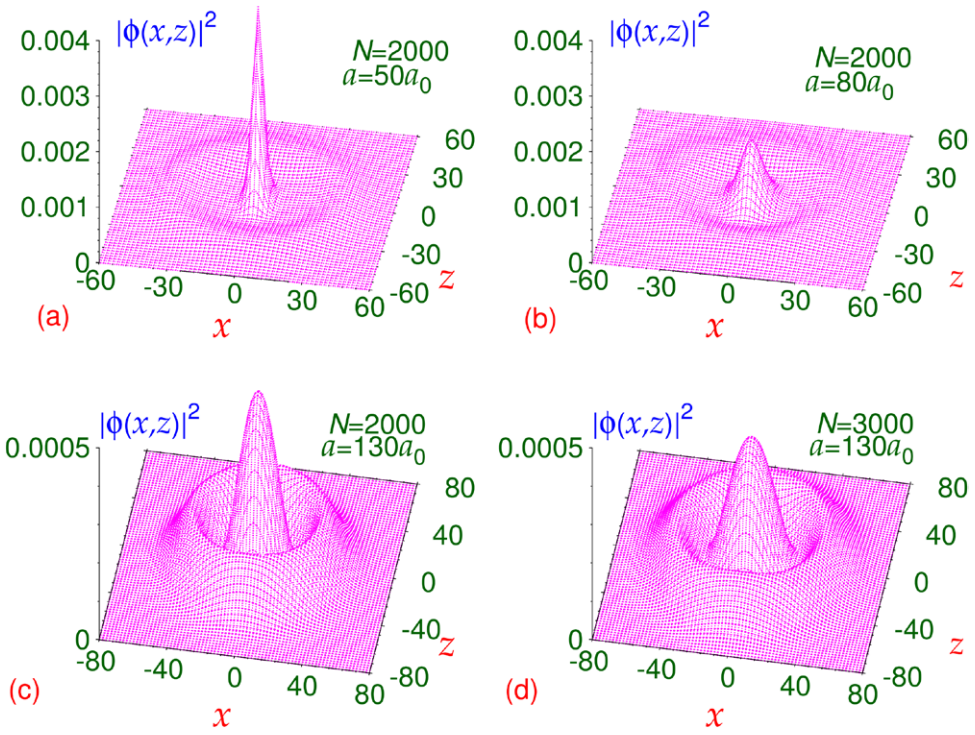

Figure 2. The density $|\phi(\vec{\rho})|^2 \equiv |\phi(x,z)|^2$ of the 2D dipolar RDB solitons for (a) $N = 2000$, $a = 50a_0$, (b) $N = 2000$, $a = 80a_0$, (c) $N = 2000$, $a = 130a_0$ and (d) $N = 3000$, $a = 130a_0$ as obtained from (4). The densities are normalised as $\int \mathrm{d}x\mathrm{d}z|\phi(x,z)|^2 = 1$ and expressed in units of l^{-2} and the length in units of l. The length scale $l = 1$ μm and the dipolar length $a_{\rm dd} = 132.7a_0$.

$$n(\mathbf{k}_\rho, t) = \int \mathrm{e}^{\mathrm{i}\mathbf{k}_\rho\cdot\vec{\rho}}|\phi_{2\mathrm{D}}(\vec{\rho},t)|^2 d\vec{\rho}, \quad \mathbf{k}_\rho \equiv (k_x, k_y), \tag{5}$$

$$j_{2\mathrm{D}}(\xi) = -1 + 3\sqrt{\pi}\frac{k_z^2}{2\xi}\mathrm{e}^{\xi^2}[1 - \mathrm{erf}(\xi)], \quad \xi = \frac{k_\rho}{\sqrt{2}}. \tag{6}$$

In this case $\int|\phi_{2\mathrm{D}}(\vec{\rho},t)|^2\mathrm{d}\vec{\rho} = 1$.

3. Numerical results

We solve the 3D equation (3) or the 2D equation (4) by the split-step Crank–Nicolson discretisation scheme using real-time propagation in 3D or 2D Cartesian coordinates, respectively, using a space step of $0.1 \sim 0.2$ and a time step of $0.0002 \sim 0.002$ in real-time simulation [28, 30]. A small time step is employed in the real-time propagation to obtain reliable and accurate results. The dipolar potential term is treated by a Fourier transformation to the momentum space using a convolution rule [31].

In 2D, the simulation is started with the normalised excited state

$$\phi_{2\mathrm{D}}(\vec{\rho}) = \sqrt{\frac{\kappa}{\pi}}[\kappa(x^2+z^2) - 1]\mathrm{e}^{-\kappa(x^2+z^2)/2} \tag{7}$$

with eigenvalue 3κ of (4) with $g = g_{\rm dd} = 0$ and harmonic trap $\kappa^2(x^2+z^2)/2$. In 3D, the excited state

$$\phi(\mathbf{r}) = \sqrt{\frac{\kappa}{\pi^{3/2}}}[\kappa(x^2+z^2) - 1]\mathrm{e}^{-\kappa(x^2+z^2)/2 - y^2/2} \tag{8}$$

with eigenvalue $3\kappa + 1/2$ of (3) with $g = g_{\rm dd} = 0$ and harmonic trap $\kappa^2(x^2+z^2)/2 + y^2/2$ is used. States (7) and (8) have a circular notch at $\rho \equiv \sqrt{x^2+z^2} = \sqrt{1/\kappa}$. The stationary profile of the quasi-2D RDB solitons can be obtained by real-time simulation. The 2D dipolar RDB solitons are excited states of 2D bright solitons and are not accessible by imaginary-time propagation, which is designed to converge to the ground states of (3) and (4). The real-time simulation is started with a small κ ($\sim$0.0025) corresponding to a circular notch at $\rho \sim 20$ and with $g = g_{\rm dd} = 0$. The final converged result is independent of the initial choice of κ, but this initial choice leads to a quick convergence of the result. In the course of simulation the nonlinearities are increased slowly to the desired values and the trap is slowly reduced to zero. In this way the real-time simulation passes through eigenstates of the GP equation until we finally reach the stable RDB soliton with a circular notch as our final state.

In this study we consider 2D RDB solitons in a BEC of ^{164}Dy atoms with magnetic moment $\mu = 10\,\mu_{\rm B}$ [17], where $\mu_{\rm B}$ is the Bohr magneton. The ^{164}Dy atoms have the largest magnetic moment among those used in dipolar BEC experiments and a large dipole moment is fundamental for achieving 2D RDB solitons with a large number of atoms. The dipolar length in this case is $a_{\rm dd} = \mu_0\mu^2 m/(12\pi\hbar^2) = 132.7a_0$ where a_0 is the Bohr radius. We take the length scale $l = 1$ μm, corresponding to a harmonic trap frequency of $\omega = 2\pi \times 61.6$ Hz along the y direction and, consequently, the time scale $t_0 = 2.6$ ms.

We study the domain of the appearance of the 2D bright solitons of (4). These solitons for a specific scattering length

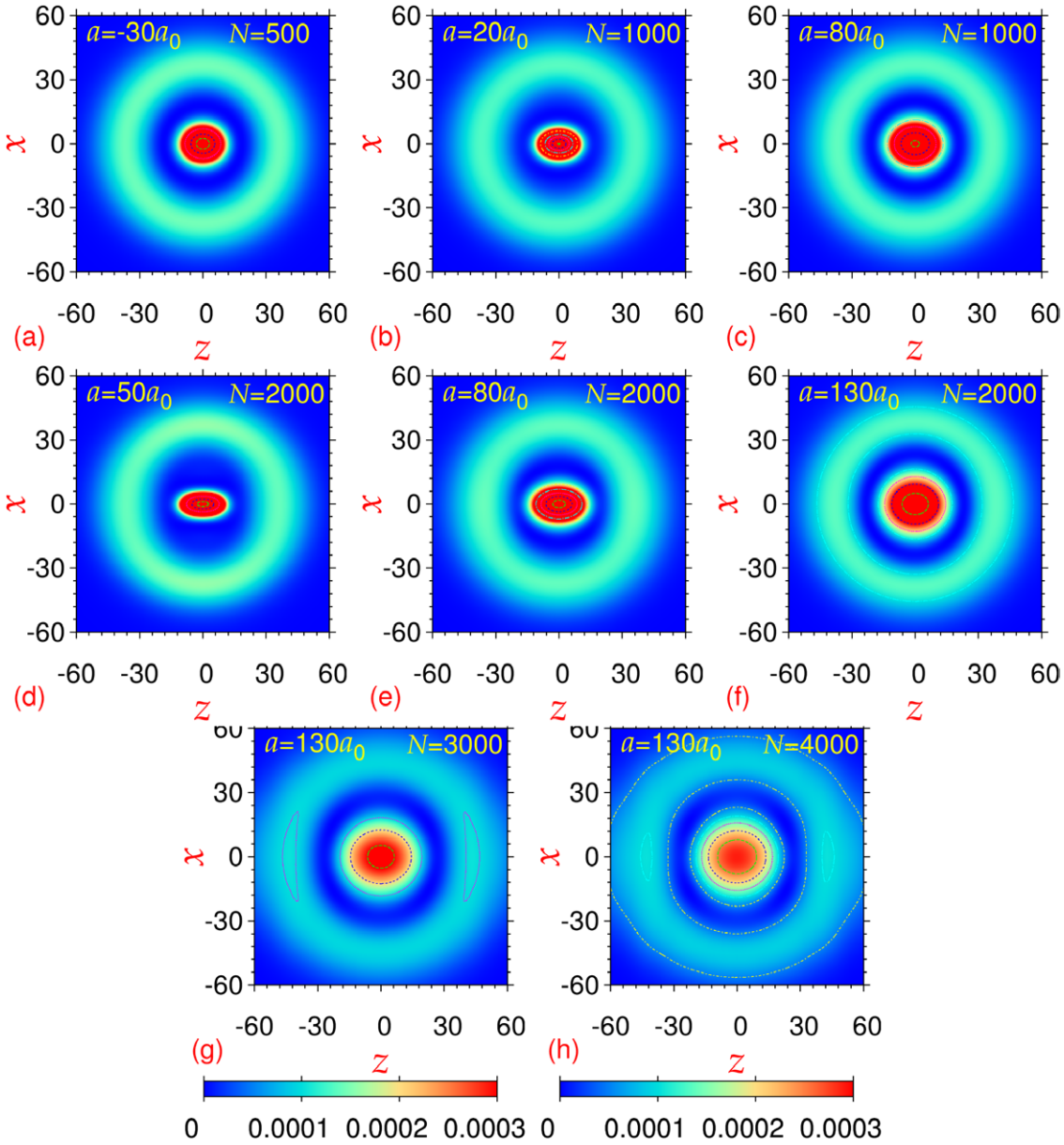

Figure 3. The contour plot of normalised density $|\phi(\vec{\rho})|^2 \equiv |\phi(x,z)|^2$ of the 2D RDB solitons from a solution of (4) for (a) $N = 500$, $a = -30a_0$, (b) $N = 1000$, $a = 20a_0$, (c) $N = 1000$, $a = 80a_0$, (d) $N = 2000$, $a = 50a_0$, (e) $N = 2000$, $a = 80a_0$, (f) $N = 2000$, $a = 130a_0$, (g) $N = 3000$, $a = 130a_0$ and (h) $N = 4000$, $a = 130a_0$. The densities are expressed in units of l^{-2} and the length in units of l and the length scale $l = 1$ μm.

can exist for the number of atoms N below a critical number $N_{\rm crit}$, beyond which the system collapses [32]. In figure 1 we plot this critical value $N_{\rm crit}$ versus a/a_0 from imaginary-time simulation. The 2D dipolar RDB solitons, as obtained by real-time simulation, have a much larger spatial extension compared to the bright solitons and can accommodate a larger number of atoms, as can be seen in figure 1. For $N > N_{\rm crit}$, the soliton collapses due to an excess of dipolar attraction. In the stable region there is a balance between attraction and repulsion to form the bright soliton. The number of atoms in the 2D dipolar bright and RDB solitons could be quite large and will be of experimental interest. The size of quasi-1D nondipolar solitons is usually quite small and accommodates only a small number of atoms.

Next we present the profile of the 2D RDB solitons as obtained from (4) by real-time propagation for a different number of ^{164}Dy atoms and different scattering lengths. The scattering length can be adjusted to a desired value by the magnetic [33] and optical [34] Feshbach resonance technique. The densities of the different RDB solitons for (a) $N = 2000$, $a = 50a_0$, (b) $N = 2000$, $a = 80a_0$, (c) $N = 2000$, $a = 130a_0$ and (d) $N = 3000$, $a = 130a_0$, are shown in figure 2. A Gaussian input wave function converges to the 2D bright soliton studied in [21]. The input functions (7) and (8) in (3) and (4), respectively, with a circular notch at $\rho = 1/\sqrt{\kappa}$ representing a radial excitation, converge to the RDB soliton profiles shown in figure 2. Due to the anisotropic dipolar interaction, the densities of the RDB solitons are anisotropic on the

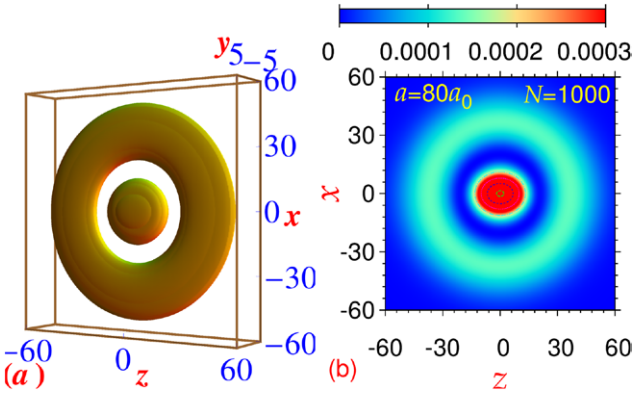

Figure 4. (a) Isodensity profile of the 2D RDB soliton obtained from a solution of the 3D GP equation (3) for $N = 1000$ and $a = 80a_0$. The 3D contour is set at 0.00002. (b) The contour plot of the quasi-2D density $|\phi_{2D}(x,z)|^2 = \int dy |\phi(\mathbf{r})|^2$ of the 3D calculation.

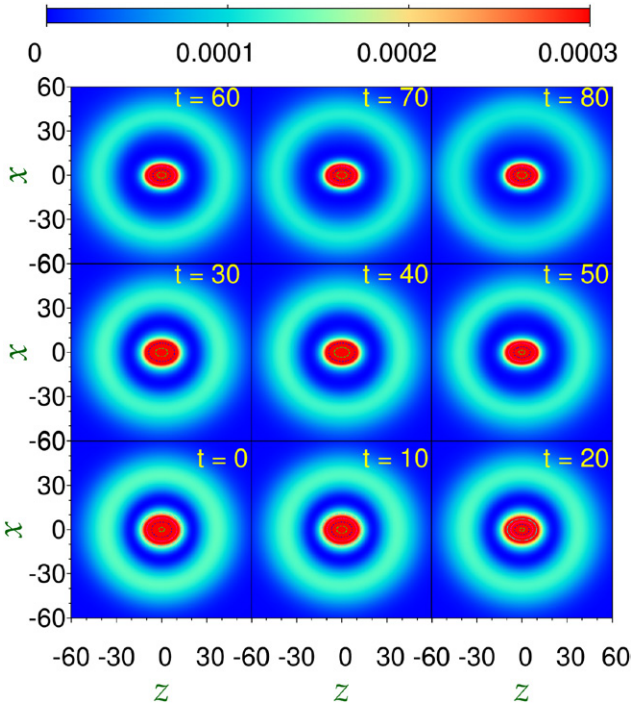

Figure 5. Contour plot of density at different times t as obtained from (4) illustrating the dynamics of a RDB soliton of 1000 ^{164}Dy atoms of scattering length $a = 80a_0$ when at $t = 0$ the scattering length is suddenly changed to $a = 20a_0$. The simulation is started with the wave function of the RDB soliton exhibited in figure 3(c).

$x - z$ plane when the dipolar interaction dominates the contact interaction ($a_{dd} \gg a$). Although the notch in the density of the RDB soliton can clearly be seen in plots of figure 2, the anisotropic shapes of the densities can be clearly seen in the contour plots of densities and this is why we consider the contour plots of density in the following.

In figure 3 we display the contour plots of the density of 2D RDB solitons for s different number N of ^{164}Dy atoms and scattering lengths a. From figures 2 and 3 and other calculations not presented here, several aspects of the density profiles of the RDB solitons are clear. For a small number of atoms

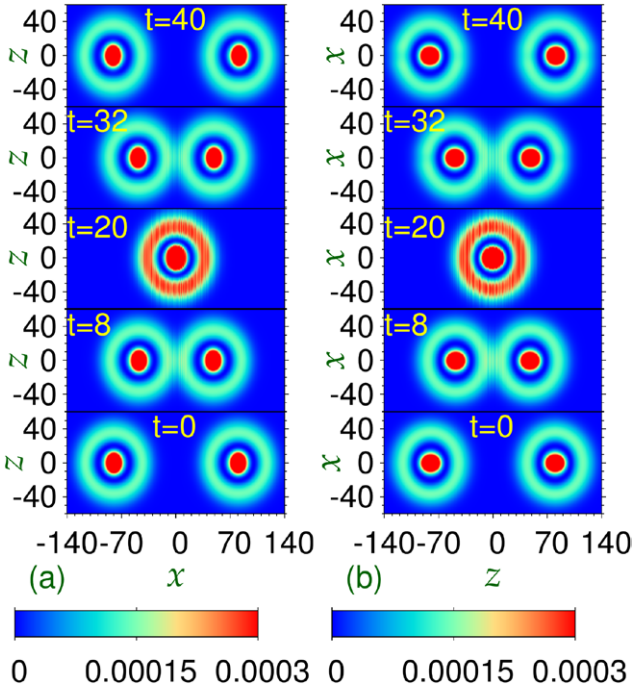

Figure 6. Contour plot of density at different times t as obtained from (4) illustrating the quasi-elastic collision of two RDB solitons of 1000 ^{164}Dy atoms of scattering length $a = 80a_0$ moving in opposite directions along the (a) x and (b) y axes, respectively, with a dimensionless velocity of four units. With the length scale $l = 1$ μm the velocity of each RDB soliton is about 1.5 mm s^{-1}.

($N < 1000$) the dipolar nonlinearity is small and consequently the density profile possesses approximate circular symmetry on the $x - z$ plane. Deviation from circular symmetry occurs for a larger number of atoms and for $a_{dd} \gg a$ when the dipolar interaction plays a dominating role in the formation of the RDB solitons. Comparing figures 3(c) and (e) for 1000 and 2000 atoms with scattering length $a = 80a_0$, we see that the anisotropy is larger for a larger number of atoms. Comparing figures 3(d)–(f) for $a = 50a_0, 80a_0$ and $130a_0$, respectively, for $N = 2000$ we find that the anisotropy has reduced with an increase in the scattering length a from $a = 50a_0$ to $130a_0$. For $a = 130a_0 \approx a_{dd} = 132.7a_0$, the anisotropic dipolar interaction plays a less dominating role in the formation of the RDB soliton and hence results in a reduced anisotropy in figures 3(f)–(h) for $N = 2000$, 3000 and 4000.

The results reported in this letter are performed with the quasi-2D GP equation (4). Although this seems very reasonable in the presence of a strong trap in the transverse y direction, it is worth comparing these densities with those obtained from a solution of the 3D GP equation (3) and we do this in the following. We calculated the density of several of the RDB solitons illustrated in figure 3 using the 3D GP equation (4). The quasi-2D densities obtained from the 2D and 3D GP equations are very similar in all cases. In figure 4(a) we show the 3D isodensity profile of the RDB soliton obtained from (3) for $N = 1000$ and $a = 80a_0$. The quasi-2D density $|\phi_{2D}(x,z)|^2 = \int dy |\phi(\mathbf{r})|^2$ obtained from the same calculation is shown in figure 4(b). This quasi-2D density is very similar

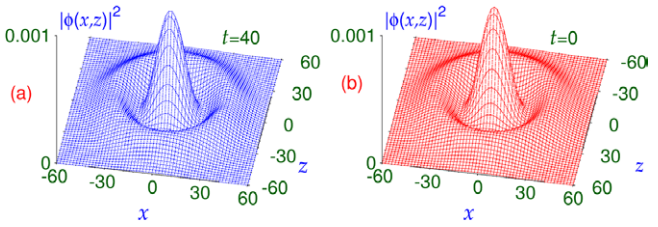

Figure 7. The (a) final ($t = 40$) and (b) initial ($t = 0$) profiles of an RDB soliton of 1000 atoms and $a = 80a_0$ undergoing collision in figure 6(b) moving along the z axis.

to the same one presented in figure 3(c) from a solution of the quasi-2D GP equation (4), which validates the use of this equation.

The 2D RDB solitons presented in figures 2 and 3 are stable and robust, as tested under real-time propagation with a reasonable perturbation in the parameters. The robustness comes from the large contact repulsion, which inhibits collapse. Also, the predominant long-range dipolar attraction on the $x - z$ plane prevents the leakage of the atoms to infinity. In a nondipolar quasi-1D BEC soliton, the contact attraction alone provides the binding and there is no repulsion to stop the collapse. We provide below two numerical tests for the stability of a RDB soliton.

First we test the stability of an RDB soliton under a sudden change in the scattering length. We perform real-time simulation, with the wave function of the RDB soliton of figure 3(c) as the initial state, when at time $t = 0$ the scattering length is suddenly changed from $a = 80a_0$ to $20a_0$. The contour plots of density at different times is exhibited in figure 5. Although the notch in the density remains intact, at large times the RDB soliton adjusts to the shape with $a = 20a_0$ shown in figure 3(b). The anisotropy has increased with time due to an increased contribution of dipolar interaction as the contact interaction is reduced at $t = 0$.

A stringent test of the robustness of these 2D RDB solitons is provided in their behaviour under head-on collision. Like the 1D dipolar solitons [20], the collision of the RDB solitons is expected to be quasi-elastic with the solitons emerging with little deformation after collision at medium velocities. Only the collision between two integrable 1D solitons is known to be perfectly elastic at all velocities [2]. We consider a head-on collision between two 2D RDB solitons in figure 3(c) moving in opposite directions along both the x and z axes. The collision dynamics of these two solitons as generated from a real-time simulation of equation (4) is shown in figure 6(a) and (b), respectively. The initial velocities of the two solitons are attributed by multiplying the initial wave functions of the two solitons by phase factors $\exp(\pm iv_x x)$, $v_x = 20$. The two 2D dipolar RDB solitons are initially placed at $x \equiv x_0 = \pm 80$ and the real-time simulation started. The two solitons move in opposite directions and suffer a head-on collision. The collision dynamics for velocity along the x direction is illustrated by plotting the density of the system at different times, as shown in figure 6(a). The dimensionless velocity of each soliton is about 4, which corresponds to about 1.5 mm/s using scales $l = 1$ μm and $t_0 = 2.6$ ms. In figure 6(b) we show the collision

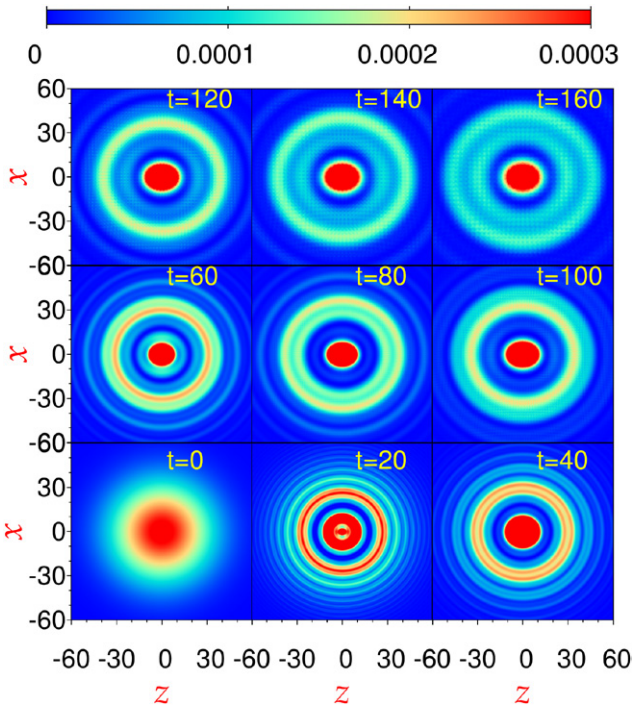

Figure 8. The contour plot of density at different times during real-time simulation using equation (4) with $N = 1000$ and $a = 80a_0$ with the hase imprinted profile (9) and (10) with $\kappa = 0.001$ and $\rho_0 = 18$ as the initial state.

dynamics for velocity along the z direction. The smooth density profiles of the dynamics presented in figure 6 illustrates the quasi-elastic nature of the dynamics. In figure 7(a) we plot the final density of one of the solitons after the collision at $t = 40$ shown in figure 6(b) and compare it with the initial density before the collision shown in figure 7(b). The similarity between the two densities shown in figure 7 illustrates the quasi-elastic nature of the collision.

As the 2D dipolar RDB solitons are stable and robust, they can be prepared from the phase-imprinted [26] Gaussian profile

$$\phi_{2D}(\vec{\rho}) = \sqrt{\frac{\kappa}{\pi}}\, e^{-\kappa(x^2+z^2)/2}, \quad \rho < \rho_0, \tag{9}$$

$$= -\phi_{2D}(\vec{\rho}), \quad \rho \geqslant \rho_0, \tag{10}$$

in the trapless case. In an experiment a homogeneous potential generated by the dipole potential of a far detuned laser beam should be applied on part of the Gaussian profile ($\rho < \rho_0$) for an interval of time so as to imprint an extra phase of π on the wave function for $\rho < \rho_0$ [4]. The thus phase-imprinted Gaussian profile with $\kappa = 0.001$, $\rho_0 = 18$ is propagated in real time with $N = 1000$ and $a = 80a_0$, while it slowly transforms into a 2D dipolar RDB soliton. This simulation is done with no trap. In actual experiment a very weak in-plane trap can be kept during generating the 2D RDB soliton, which can be eventually removed. The simulation is shown in figure 8, where we show the density at different times. It is illustrated that at large times the density evolves towards that of the 2D RDB soliton shown in figure 3(c).

4. Summary

We demonstrated the possibility of creating a mobile, stable 2D RDB soliton, in a dipolar quasi-2D BEC of ^{164}Dy atoms polarised along the z axis and trapped along the y axis, with a circular notch and capable of moving on the $x - z$ plane at a constant velocity. The 2D RDB solitons are stationary solutions of the mean-field GP equation. The stability of the RDB soliton is established from a prolonged real-time simulation after a sudden change in the scattering length. The head-on collision between two such solitons with a relative velocity of about 1.5 mm s^{-1} is quasi-elastic with the solitons passing through each other with practically no deformation. A possible way of preparing these 2D dipolar RDB solitons by phase imprinting a Gaussian profile is demonstrated using real-time propagation. The results and conclusions of this letter can be tested in experiments with present-day know-how and technology and should lead to interesting future investigations.

Acknowledgments

We thank the Fundação de Amparo à Pesquisa do Estado de São Paulo (Brazil, Project No. 2012/00451-0) and the Conselho Nacional de Desenvolvimento Científico e Tecnológico (Brazil, Project No. 303280/2014-0) for partial support.

References

[1] Kivshar Y S and Malomed B A 1989 *Rev. Mod. Phys.* **61** 763
Abdullaev F K, Gammal A, Kamchatnov A M and Tomio L 2005 *Int. J. Mod. Phys.* B **19** 3415
[2] Strecker K E, Partridge G B, Truscott A G and Hulet R G 2002 *Nature* **417** 150
Khaykovich L, Schreck F, Ferrari G, Bourdel T, Cubizolles J, Carr L D, Castin Y and Salomon C 2002 *Science* **256** 1290
[3] Cornish S L, Thompson S T and Wieman C E 2006 *Phys. Rev. Lett.* **96** 170401
[4] Burger S, Bongs K, Dettmer S, Ertmer W, Sengstock K, Sanpera A, Shlyapnikov G V and Lewenstein M 1999 *Phys. Rev. Lett.* **83** 5198
Dutton Z, Budde M, Slowe C and Hau L V 2001 *Science* **293** 663
[5] Denschlag J *et al* 2000 *Science* **287** 97
[6] Anderson B P, Haljan P C, Regal C A, Feder D L, Collins L A, Clark C W and Cornell E A 2001 *Phys. Rev. Lett.* **86** 2926
[7] Frantzeskakis D J 2010 *J. Phys. A: Math. Gen.* **43** 213001
Busch Th and Anglin J R 2000 *Phys. Rev. Lett.* **84** 2298
Fedichev P O, Muryshev A E and Shlyapnikov G V 1999 *Phys. Rev.* A **60** 3220
[8] Muryshev A, Shlyapnikov G V, Ertmer W, Sengstock K and Lewenstein M 2002 *Phys. Rev. Lett.* **89** 110401
[9] Becker C, Stellmer S, Soltan-Panahi P, Dörscher S, Baumert M, Richter E-M, Kronjäger J, Bongs K and Sengstock K 2008 *Nat. Phys.* **4** 496
Shomroni I, Lahoud E, Levy S and Steinhauer J 2009 *Nat. Phys.* **5** 193
[10] Feder D L, Pindzola M S, Collins L A, Schneider B I and Clark C W 2000 *Phys. Rev.* A **62** 053606
[11] Theocharis G *et al* 2003 *Phys. Rev. Lett.* **90** 120403
[12] Kivshar Y S and Yang X 1994 *Phys. Rev.* E **50** R40
Frantzeskakis D J and Malomed B A 1999 *Phys. Lett.* A **264** 179
Zhang J-F, Wu L, Li L, Mihalache D and Malomed B A 2010 *Phys. Rev.* A **81** 023836
[13] Neshev D, Dreischuh A, Kamenov V, Stefanov I, Dinev S, Fliesser W and Windholz L 1997 *Appl. Phys.* B **64** 429
[14] Wang W *et al* 2015 *Phys. Rev.* A **92** 033611
Hu X-H, Zhang X-F, Zhao D, Luo H-G and Liu W M 2009 *Phys. Rev.* A **79** 023619
Toikka L A and Suominen K-A 2013 *Phys. Rev.* A **87** 043601
[15] Song S-W, Wang D-S, Wang H and Liu W M 2012 *Phys. Rev.* A **85** 063617
[16] Lu M, Youn S H and Lev B L 2010 *Phys. Rev. Lett.* **104** 063001
[17] Lu M, Burdick N Q, Youn S H and Lev B L 2011 *Phys. Rev. Lett.* **107** 190401
[18] Aikawa K, Frisch A, Mark M, Baier S, Rietzler A, Grimm R and Ferlaino F 2012 *Phys. Rev. Lett.* **108** 210401
[19] Lahaye T *et al* 2007 *Nature* **448** 672
Koch T, Lahaye T, Metz J, Fröhlich B, Griesmaier A and Pfau T 2008 *Nat. Phys.* **4** 218
[20] Young-S L E, Muruganandam P and Adhikari S K 2011 *J. Phys. B: At. Mol. Opt. Phys.* **44** 101001
[21] Nath R, Pedri P and Santos L 2009 *Phys. Rev. Lett.* **102** 050401
Tikhonenkov I I, Malomed B A and Vardi A 2008 *Phys. Rev. Lett.* **100** 090406
Köberle P, Zajec D, Wunner G and Malomed B A 2012 *Phys. Rev.* A **85** 023630
[22] Adhikari S K and Muruganandam P 2012 *Phys. Lett.* A **376** 2200
[23] Adhikari S K and Muruganandam P 2012 *J. Phys. B: At. Mol. Opt. Phys.* **45** 045301
Tikhonenkov I, Malomed B A and Vardi A 2008 *Phys. Rev.* A **78** 043614
[24] Adhikari S K *Phys. Rev.* A 2014 **89** 043615
[25] Adhikari S K 2014 *J. Phys. B: At. Mol. Phys.* **47** 225304
[26] Dobrek L, Gajda M, Lewenstein M, Sengstock K, Birkl G and Ertmer W 1999 *Phys. Rev.* A **60** R3381
[27] Lahaye T, Menotti C, Santos L, Lewenstein M and Pfau T 2009 *Rep. Prog. Phys.* **72** 126401
[28] Kishor Kumar R, Young-S L E, Vudragovic D, Balaz A, Muruganandam P and Adhikari S K 2015 *Comput. Phys. Commun.* **195** 117
[29] Muruganandam P and Adhikari S K 2012 *Laser Phys.* **22** 813
Fischer U R 2006 *Phys. Rev.* A **73** 031602
Pedri P and Santos L 2005 *Phys. Rev. Lett.* **95** 200404
[30] Muruganandam P and Adhikari S K 2009 *Comput. Phys. Commun.* **180** 1888
Vudragović D, Vidanovic I, Balaž A, Muruganandam P and Adhikari S K 2012 *Comput. Phys. Commun.* **183** 2021
Loncar V, Balaz A, Bogojevic A, Skrbic S, Muruganandam P and Adhikari S K 2016 *Comput. Phys. Commun.* **200** 406
Satari C B, Slavnic V, Belic A, Balaz A, Muruganandam P and Adhikari S K 2016 *Comput. Phys. Commun.* **200** 411
[31] Goral K and Santos L 2002 *Phys. Rev.* A **66** 023613
[32] Ronen S, Bortolotti D C E and Bohn J L 2007 *Phys. Rev. Lett.* **98** 030406
[33] Inouye S *et al* 1998 *Nature* **392** 151
[34] Fedichev P O, Kagan Yu, Shlyapnikov G V and Walraven J T M 1996 *Phys. Rev. Lett.* **77** 2913